

A solution to the subdiffusion-efficiency paradox: Inactive states enhance reaction efficiency at subdiffusion conditions in living cells

LEILA ESMAEILI SERESHKI¹, MICHAEL A. LOMHOLT² and RALF METZLER^{3,4} (a)

¹ Department of Physics, Technical University of Munich, James-Frank Straße, 85747 Garching, Germany

² MEMPHYS - Center for Biomembrane Physics, Department of Physics, Chemistry and Pharmacy, University of Southern Denmark, Campusvej 55, 5230 Odense M, Denmark

³ Institute for Physics and Astronomy, University of Potsdam, D-14476 Potsdam-Golm, Germany

⁴ Department of Physics, Tampere University of Technology, FI-33101 Tampere, Finland

PACS 05.40.-a – Fluctuation phenomena, random processes, noise, and Brownian motion

PACS 87.10.-e – General theory and mathematical aspects

PACS 87.16.-b – Subcellular structure and processes

PACS 87.18.-h – Biological complexity

Abstract –Macromolecular crowding in living biological cells effects subdiffusion of larger biomolecules such as proteins and enzymes. Mimicking this subdiffusion in terms of random walks on a critical percolation cluster, we here present a case study of EcoRV restriction enzymes involved in vital cellular defence. We show that due to its so far elusive propensity to an inactive state the enzyme avoids non-specific binding and remains well-distributed in the bulk cytoplasm of the cell. Despite the reduced volume exploration capability of subdiffusion processes, this mechanism guarantees a high efficiency of the enzyme. By variation of the non-specific binding constant and the bond occupation probability on the percolation network, we demonstrate that reduced non-specific binding are beneficial for efficient subdiffusive enzyme activity even in relatively small bacteria cells. Our results corroborate a more local picture of cellular regulation.

Introduction. – Diffusion-limited biochemical cellular reactions underlying signalling and regulation processes have traditionally been investigated at dilute solvent conditions [1]. The relevance of this picture for diffusion control in living cells has been challenged in view of *macromolecular crowding*, the occupation of a considerable volume fraction f of the cellular cytoplasm by larger biopolymers [2]. Estimates for f typically range from 35% to 40%. Bearing in mind that on a cubic lattice the site percolation threshold is $f \approx 31\%$ and that of bond percolation $f \approx 25\%$ [4, 5], molecular crowding may indeed appear severe. Crowding effects changes in enzyme function and turnover, as well as protein folding and aggregation [3, 6].

Larger biopolymers and tracers in living biological cells and artificially crowded control environments perform subdiffusion of the form [7–15]

$$\langle \mathbf{r}^2(t) \rangle \simeq t^\alpha \text{ with } 0 < \alpha < 1, \quad (1)$$

as observed experimentally for particles as small as 10 kD,

with α in the range of 0.40 to 0.90 [8, 9, 11, 13, 14], in accord with recent high-detail simulations [6]. The observed subdiffusion has been measured to persist over tens to hundreds of seconds [9, 11] and thus appears relevant to cellular processes such as gene regulation or molecular defence mechanisms. Subdiffusion leads to reduced global volume exploration, to dynamic localisation at reactive interfaces [18], and may prevent chromosomal mixing in eukaryotic nuclei [10]. It has been argued that subdiffusion may in fact be beneficial for cellular processes, by increasing the probability to find, and react with a *nearby* target [9, 16]. In that sense subdiffusion would give rise to a more local picture of diffusion-limited biochemical reactions in biological cells, see below.

Here we study by simulations the reaction dynamics of EcoRV restriction enzymes in *Escherichia coli* (*E.coli*) bacteria. EcoRV in solution forms homodimers of molecular weight 58 kD [24], and thus belongs to the range of sizes for which subdiffusion (1) under crowding was reported [6, 8, 13]. Our results show that despite the subdiffusion control EcoRV's performance is surprisingly high. This

(a) E-mail: rmetzler@uni-potsdam.de

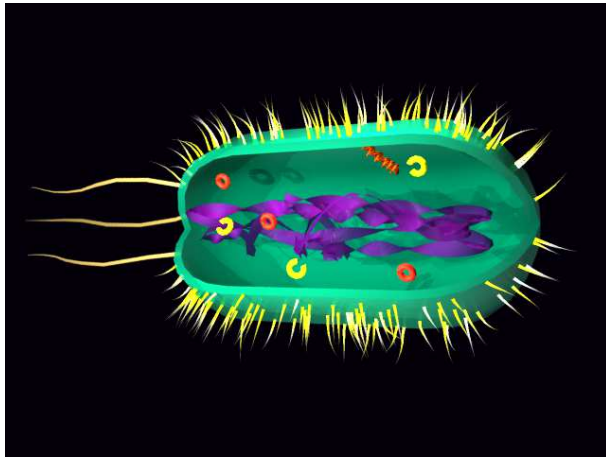


Figure 1: Sketch of an *E.coli* cell with native DNA (violet) concentrated in the centre. EcoRV restriction enzymes occur in two isomers: inactive, with closed cleft (red), and active with open cleft (yellow). Invading, foreign DNA (red double-helix) is attacked by EcoRV and cut. The void intracellular space shown here in reality is crowded by larger biopolymers.

provides a concrete solution to the subdiffusion-efficiency paradox and supports current ideas that subdiffusion does not contradict efficient molecular reactions in cells.

EcoRV enzymes and our model approach.

The type II restriction endonuclease EcoRV binds non-specifically to double-stranded DNA. Once it locates its specific six-base sequence 5'-GAT|ATC-3' it cuts the double-strand and renders it inactive. This is an important mechanism in the cellular defence against alien DNA stemming from, e.g., viruses attacking the cell [19]. The cell's native DNA is protected against EcoRV by methylation of the DNA at cytosine or adenine [20]. Interestingly, EcoRV is found in two configurations [21, 22]: as seen by X-ray crystallography, the unbound protein may switch between an inactive structure with a closed cleft and another, in which the cleft is more open. In the open, active state EcoRV binds both non-specifically to DNA and specifically to its cognate binding site.

In Fig. 1 we sketch an *E.coli* cell and its native DNA, EcoRV enzymes in active and inactive states being either attached non-specifically to the native DNA or freely diffusing in the cellular cytoplasm. The apparent void space in reality is a highly crowded ('superdense' [9]) complex liquid, in which the enzymes subdiffuse. An invading DNA is being recognised and cleaved by active EcoRV enzymes.

Remarkably, the probability x_{act} to find the enzyme in the open-cleft, active state at a given instant of time is as low as $\sim 1\%$ [23]. It is a priori puzzling why a vital defence mechanism should be equipped with such a low activity. A physiologic rationale of the open/closed isomerisation could be to reduce non-specific binding to the cell's native DNA. Alien DNA invading the cell would thus immediately be surrounded by a higher EcoRV concentra-

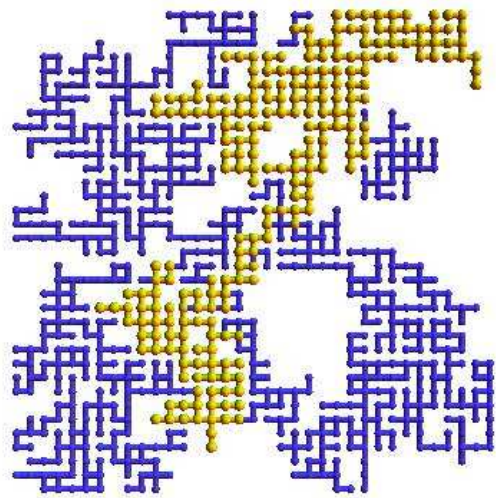


Figure 2: Diffusion trace (yellow) on a bond percolation cluster.

tion that, after switching to the active state, could attack this DNA [23]. Our results show, however, under the assumption of normal diffusion in the cell the performance of EcoRV is only marginally better than that of a 100%-active mutant: normal diffusion on the length scales of an *E.coli* cell provides very efficient mixing, and the reduced activity of EcoRV would not constitute an advantage. As we will show this situation changes drastically under subdiffusion, and low activity in fact becomes advantageous.

Following previous studies [27–30] we model the subdiffusion of EcoRV enzymes as random walks on a critical percolation cluster. The use of a fractal medium is in line with observations that the crowded cytoplasm may have a random fractal structure [25]. The lattice spacing is chosen as the size of an EcoRV. A bond between lattice points is created with occupation probability p . If $p = 1$ the entire lattice is accessible and the diffusion is normal. Reducing p to the critical value $p_c = 0.2488$ or slightly above, the resulting cluster of permitted bonds is fractal with dimension $d_f \approx 2.58$ and the diffusion becomes anomalous with $\alpha \approx 0.51$. From extensive lattice simulations (see Appendix) we sample the times an enzyme needs to locate its target, a specific sequence on an invading stretch of DNA randomly positioned in the cellular cytoplasm (the volume not occupied by the native DNA). The average target knockout time, equivalent to the mean first passage time (MFPT) to hit the target in an active state, is studied as function of the bond occupation probability p and the non-specific binding constant K_{ns}^0 of active EcoRV to DNA.

Fig. 2 depicts part of the spanning percolation cluster and part of a random walk trace on this cluster. Due to the reduced connectivity in the fractal cluster, the trajectory reflects the existence of holes existing on all scales. The appearance of dead ends and bottlenecks in the scale-free environment effects subdiffusion [4].

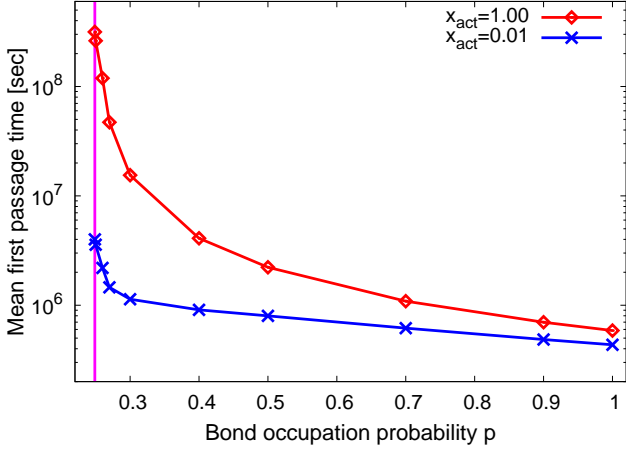


Figure 3: Typical time for the restriction enzyme to locate the target in an active state (MFPT) on a cubic lattice, as function of the bond occupation probability. Close to criticality ($p_c = 0.2488$ is marked by the vertical line), subdiffusion emerges with anomalous diffusion exponent $\alpha = 0.51$. The non-specific binding constant is $K_{ns}^0 = 10^7$ [$M^{-1}bp^{-1}$] [26]. Error bars are of the size of the symbols or less.

Simulations results. — In Fig. 3 we compare the MFPT for EcoRV (activity $x_{act} = 0.01$) and mutant enzyme ($x_{act} = 1$) versus the bond occupation probability p , ranging from full occupation ($p = 1$, normal diffusion) down to the percolation threshold $p = 0.2488$ (subdiffusion with $\alpha = 0.51$). For normal diffusion ($p = 1$) the MFPT is just a factor of two smaller for EcoRV, compared to the fully active mutant. Approaching the percolation threshold the native EcoRV increasingly outperforms the mutant, at criticality EcoRV’s MFPT is *two orders of magnitude* shorter than that of the mutant.

On average, the concentration of EcoRV is approximately $1/x_{act} = 100$ times higher in the cytoplasm outside the volume of the cell’s native DNA than that of the mutant enzyme. At criticality, it is time-costly to cover distances, and thus EcoRV is 100 times more efficient than the fully active mutant enzymes. The latter become trapped around the native DNA, to which they bind non-specifically. In contrast, under normal diffusion conditions ($p = 1$) spatial separation is hardly significant, and the lower concentration is compensated by the higher activity of the mutant.

In absolute numbers, even under severe anomalous diffusion with $\alpha \approx 0.51$ EcoRV’s MFPT is only a factor of ten higher than at normal diffusion. That means that the low-activity property of EcoRV renders their efficiency almost independent of the diffusion conditions, compared to the huge difference observed for the mutant. The highly increased relative performance of the native EcoRV is the central result of this study. It demonstrates that subdiffusion is not prohibiting efficient molecular reactions. Moreover, our result provides a novel rationale for

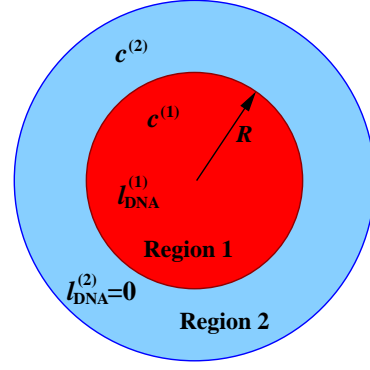


Figure 4: Sketch of the cross section of an *E.coli* model cell. Region 1 contains the cell’s native DNA. In Region 2 (“cytoplasm”), foreign target DNA are attacked by active restriction enzymes. The various symbols are explained in the text.

EcoRV’s elusive low-activity, that in this light appears as a designed property. We note that the MFPT shown here is the result for an individual EcoRV enzyme. Typically, a bacteria cell combines a fairly large number of restriction enzymes of various families. This significantly reduces the time scales indicated here, while preserving the characteristics of the EcoRV superiority.

Discussion. — To obtain a better physical understanding of the rôle played by events of EcoRV non-specific binding to the cell’s native DNA, we study the dependence of the MFPT on the non-specific binding constant K_{ns}^0 . Experimentally, K_{ns}^0 can be varied by changing the salt concentration of the solution. For the cubic lattice ($p = 1$) we obtain an analytical expression for the MFPT for the geometry sketched in Fig. 4. We distinguish Region 1 containing the native DNA, and Region 2 representing the cytoplasm, in which the foreign DNA enters and the EcoRV action occurs.

Let us first address the non-specific binding of EcoRV enzymes to the native cellular DNA in Region 1, corresponding to a volume of length of L and radius R . Assuming rapid equilibrium with respect to enzyme binding and unbinding from the DNA, we observe the following relation between the volume concentrations of bound and unbound *active* (ready-to-bind) enzymes,

$$\frac{c_{act}^{(1)}}{c_{bound}^{(1)}} = \frac{1}{K_{ns}^0 l_{DNA}^{(1)}}. \quad (2)$$

In our notation $c^{(1)}$ is the overall volume concentration of enzymes in Region 1, while $c_{bound}^{(1)}$ and $c_{bulk}^{(1)}$, respectively, measure the volume concentrations of enzymes bound to the native DNA and of unbound enzymes. The non-specific binding constant K_{ns}^0 to DNA refers to active (open-cleft) enzymes per DNA length, and is of dimension $[K_{ns}^0] = M^{-1}bp^{-1}$. Finally, $l_{DNA}^{(1)}$ is the length of DNA per volume in Region 1. Of the unbound enzymes, a fraction x_{act} is in the active (open-cleft) state, ready to bind

to DNA. Thus, the concentration of active unbound enzymes in Region 1 becomes $c_{\text{act}}^{(1)} = x_{\text{act}} c_{\text{bulk}}^{(1)}$, and one may introduce an overall binding constant $K_{\text{ns}}^0 = x_{\text{act}} K_{\text{ns}}^0$:

$$\frac{c_{\text{bulk}}^{(1)}}{c_{\text{bound}}^{(1)}} = \frac{1}{x_{\text{act}} K_{\text{ns}}^0 l_{\text{DNA}}^{(1)}} = \frac{1}{K_{\text{ns}}^0 l_{\text{DNA}}^{(1)}}. \quad (3)$$

As the total enzyme concentration in Region 1 is $c^{(1)} = c_{\text{bulk}}^{(1)} + c_{\text{bound}}^{(1)}$, and we have $c_{\text{bound}}^{(1)} = c_{\text{bulk}}^{(1)} x_{\text{act}} K_{\text{ns}}^0 l_{\text{DNA}}^{(1)}$ we can write $c_{\text{bulk}}^{(1)} = c^{(1)} / [1 + x_{\text{act}} K_{\text{ns}}^0 l_{\text{DNA}}^{(1)}]$. In Region 1 the enzyme concentration in the continuum limit will be governed by a diffusion equation of the form

$$\frac{\partial c^{(1)}}{\partial t} = D_{\text{eff}} \nabla^2 c^{(1)}, \quad (4)$$

where $D_{\text{eff}} = D_{3d} / (1 + x_{\text{act}} K_{\text{ns}}^0 l_{\text{DNA}}^{(1)})$ is an effective diffusion coefficient incorporating the assumption of rapid equilibrium with respect to binding to DNA and switching between active and dormant states. 1D diffusion along the DNA is assumed so slow that it can be ignored in connection with the overall diffusion of the enzyme. Indeed the 1D diffusion constant for EcoRV have been measured to be orders of magnitude smaller than for 3D diffusion [31].

In Region 2 we assume that 3D diffusion is fast allowing us to write a conservation law for enzymes in the form of the difference between the flux across the boundary with Region 1, and the amount of enzymes reacting with the target per time,

$$\frac{d}{dt} V^{(2)} c^{(2)} = -A^{(1)} D_{\text{eff}} \left. \frac{\partial c^{(1)}}{\partial r} \right|_{r=R} - k_a c^{(2)}. \quad (5)$$

Here $V^{(2)}$ is the volume of Region 2, $A^{(1)} = 2\pi RL$ is the surface area of Region 1, and k_a is the rate constant for reaction with the target. The x_{act} dependence of the rate k_a is $k_a = x_{\text{act}} k_a^0$, where k_a^0 is the rate constant for the active state. Note that in our approach we assume that the switching between active and dormant state is fast in comparison with the diffusion across the regions, i.e., we may assume an equilibrium between these two states. Finally, we take c_{bulk} to be continuous across the boundary between the Regions 1 and 2, and that initially the system is at equilibrium with respect to the reaction-free situation with $k_a = 0$. From the above system of equations the average search time yields in the form

$$T = \left(1 + x_{\text{act}} K_{\text{ns}}^0 l_{\text{DNA}}^{(1)}\right) \left\{ \frac{V^{(1)}}{k_a^0 x_{\text{act}}} (1 + y) + \frac{R^2}{8D_{3d}} \frac{1}{1 + y} \right\}, \quad (6)$$

where $y = V^{(2)} / [V^{(1)} (1 + x_{\text{act}} K_{\text{ns}}^0 l_{\text{DNA}}^{(1)})]$.

The simulations were carried out on a $100 \times 100 \times 100$ cubic lattice with native DNA occupying a $100 \times 50 \times 50$ lattice in the middle. To compare the present calculation with the simulations we assume a lattice spacing of $a = 10$ nm and set $L = 1 \mu\text{m}$, $V^{(2)} = 1 \mu\text{m}^3$ and thus

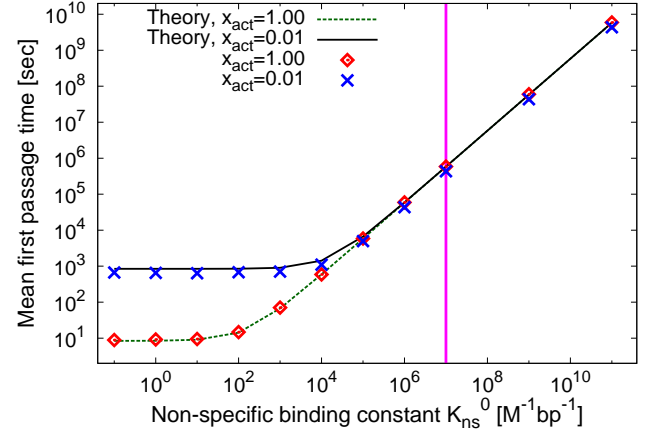


Figure 5: MFPT on a normal lattice ($p = 1$), as function of the non-specific binding constant K_{ns}^0 . Simulations results are compared to the theoretical result (6). The vertical line marks the value $K_{\text{ns}}^0 = 10^7 \text{ M}^{-1} \text{ bp}^{-1}$ used in Fig. 3.

$V^{(1)} = 0.25 \mu\text{m}^3$. From this we obtain $R = \sqrt{V^{(1)} / (\pi L)} \approx 0.28 \mu\text{m}$. Furthermore we choose the enzyme diffusivity $D_{3d} = 3 \mu\text{m}^2/\text{sec}$ [value obtained for lac repressor in vivo at short times [32]] the DNA length per volume $l_{\text{DNA}}^{(1)} = 1.5 \times 10^{-3} \text{ m}/V^{(1)}$, and $K_{\text{ns}}^0 = 10^7 \text{ M}^{-1} \text{ bp}^{-1}$, such that $K_{\text{ns}} = 10^5 \text{ M}^{-1} \text{ bp}^{-1}$ when $x_{\text{act}} = 0.01$ [33] (except for plots where this parameter is varied) with the base pair length $\text{bp} = 0.35$ nm. For the target association rate constant we take $k_a^0 = (Na)^3 / T_{\text{lattice}} = a^3 (1 - R_{3d}) / \tau_{\text{step}}$. Here $T_{\text{lattice}} = N^3 \tau_{\text{step}} / (1 - R_{3d})$ is the average search time for a random walker starting far from the target on a $N \times N \times N$ cubic lattice and spending a time τ_{step} per step to nearest neighbour sites. $R_{3d} \approx 0.340537$ is the walker's return probability to its origin [34]. Matching τ_{step} with the above diffusion constant through the mean squared displacement of the walker we obtain $\tau_{\text{step}} = a^2 / (6D_{3d}) \approx 5.6 \mu\text{s}$. The assumption of a one lattice site target gives a target size of $a = 10$ nm. We have taken this target size to be lower than the in vitro effective sliding length [23] at optimal salt conditions, partly due to possible blocking on the DNA by other DNA-binding proteins.

The above numbers yield $K_{\text{ns}}^0 l_{\text{DNA}}^{(1)} \approx 3 \times 10^5$, $y|_{x_{\text{act}}=1} \approx 10^{-5}$, $y|_{x_{\text{act}}=0.01} \approx 10^{-3}$, $V^{(1)} / k_a^0 \approx 2 \text{ sec}$, and $R^2 / (8D_{3d}) \approx 0.003 \text{ sec}$, and with these parameters we have to a good approximation $T = K_{\text{ns}}^0 l_{\text{DNA}}^{(1)} V^{(1)} / k_a^0$, regardless of whether $x_{\text{act}} = 1$ or $x_{\text{act}} = 0.01$.

The simulations results for the case of normal diffusion are displayed in Fig. 5. At small K_{ns}^0 the mutant ($x_{\text{act}} = 1$) clearly outperforms EcoRV, the gap in the MFPT corresponding to the reduced activity ($x_{\text{act}} = 0.01$). At increasing K_{ns}^0 both EcoRV and mutant perform almost identically, with a small advantage to EcoRV. In this regime almost all active enzymes are bound to the cellular DNA, such that EcoRV has approximately a factor of

$1/x_{\text{act}} = 100$ higher bulk concentration. Concurrently, its association rate constant with the target DNA in the cytoplasm is reduced by the same factor. In this normally diffusive regime dominated by non-specific binding, reduced activity of the restriction enzyme has no significant advantage. The resulting MFPT behaviour according to Eq. (6) $T \approx K_{\text{ns}}^0 \ell_{\text{DNA}}^{(1)} V^{(1)} / k_0^a$ in this regime depends linearly on the non-specific binding constant. Indeed, this behaviour is independent of x_{act} . The agreement between the theoretical model and the simulations results is excellent over the entire range of K_{ns}^0 (Fig. 5).

Fig. 6 shows the behaviour in the case of subdiffusion: almost over the entire K_{ns}^0 range, EcoRV significantly outperforms the mutant. At sufficiently large K_{ns}^0 values (above some $10^3 \text{ M}^{-1}\text{bp}^{-1}$) the value of the MFPT is approximately two orders of magnitude smaller, i.e., the performance is improved by a factor close to the value $1/x_{\text{act}}$. This behaviour is thus dominated by the costly subdiffusion from the site of non-specific binding to the target. At low K_{ns}^0 values both curves converge. Now, the MFPT is fully dominated by anomalous diffusion to the target. Due to the compactness of the diffusion on the fractal cluster the difference between EcoRV and the mutant becomes marginal: upon an unsuccessful reaction attempt, EcoRV has a higher probability to hit the target repeatedly before full escape, improving the efficiency. In Fig. 6 the thick lines show the average of simulations over three different critical percolation clusters, while the thin black lines depict the result for each individual cluster. Apart from the low K_{ns}^0 limit, the results are very robust to the shape of the individual cluster. It would be interesting to derive analytically the MFPT dependence on K_{ns}^0 . While the MFPT problem on a fractal has been solved recently [35], it is not clear how to apply this method in the present case, due to the division of the support into two subdomains. Similarly, for the related case of fractional Brownian motion [36] this remains an open question.

Conclusions. — It is often argued that molecular processes in the cell could not be subdiffusive, as this would compromise the overall fitness of the cell due to the slowness of the response to external and internal perturbations. Here we demonstrated a solution to this subdiffusion-efficiency paradox: specific molecular design renders the efficiency of EcoRV enzymes almost independent on the exact diffusion conditions. Even though EcoRV are not always ready to bind, under subdiffusion conditions the low enzyme activity represents a superior strategy.

Cellular subdiffusion may also be modelled by fractional Brownian motion (FBM) or continuous time random walks (CTRW) [37]. FBM shares many features with diffusion on fractal structures, e.g., the compactness and ergodicity. The essential observations for the MFPT found herein should therefore be similar for the case of FBM. In contrast, for CTRW subdiffusion the high probability of not moving in a given period of time will significantly enhance the advantage of EcoRV over the mutant: while

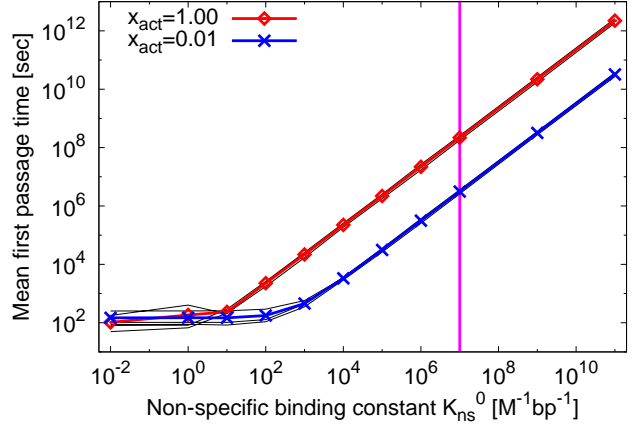


Figure 6: MFPT on a percolation cluster close to criticality ($p_c = 0.25$) versus the binding constant K_{ns}^0 . The value $K_{\text{ns}}^0 = 10^7 \text{ M}^{-1}\text{bp}^{-1}$ used in Fig. 3 is marked by the vertical line. Thick coloured lines: average over three different percolation clusters. Thin black lines: results for the individual clusters.

being trapped next to the target EcoRV would have ample chance to convert to the active state and knock out the target. It will be interesting to compare our results to simulations on a dynamic percolation cluster.

Subdiffusion-limited reactions generally increase the likelihood for biochemical reactions to occur when the reactants are close-by [9, 16]. Such a more local picture of cellular biomolecular reactions in fact ties in with the observed colocalisation of interacting genes [17]. In higher cells the similar locality is effected by internal compartmentalisation by membranes. It will be interesting to obtain more detailed information from single particle tracking experiments in living cells, in order to develop an integrated theory for cellular signalling and regulation under crowding conditions in living cells.

Financial support from the Deutsche Forschungsgemeinschaft, the Center for Nanoscience, the Academy of Finland (FiDiPro scheme), and the Danish National Research Foundation is gratefully acknowledged.

Appendix. — Our simulations of the search process were carried out on a $100 \times 100 \times 100$ cubic lattice. We considered bond percolation, i.e., for each pair of nearest neighbour sites a bond is constructed with a probability p . The searching random walker is only allowed to walk between connected sites (compare Fig. 2). The largest cluster of connected sites was chosen and the remaining sites discarded. Of these remaining sites those within the central $100 \times 50 \times 50$ -size part constitute Region 1 with the native DNA. The number of such sites is denoted by $N^{(1)}$ and the volume of this region is thus $V^{(1)} = a^3 N^{(1)}$. The remaining sites outside this region constitute the cyto-

plasm. The number of these sites is $N^{(2)}$, and the corresponding volume becomes $V^{(2)} = a^3 N^{(2)}$. A single target site is chosen randomly among the cytoplasm sites.

The initial position of the searching random walker is chosen by first deciding whether it is bound or unbound. With probability $(V^{(1)} + V^{(2)})/[V^{(2)} + V^{(1)}(1 + x_{\text{act}}K_{\text{ns}}^0I_{\text{DNA}}^{(1)})]$ it is chosen to be unbound. In this case its initial position is chosen randomly among all $N^{(1)} + N^{(2)}$ sites, and with probability x_{act} it is chosen to be in the active state (otherwise it is in the inactive state). If the walker is initially chosen to be bound, then it is placed randomly among the native DNA sites, and its state is initially set as active.

The initial time is set to $t = 0$, and the search is carried out according to the following algorithm:

1. If the walker is in the inactive state or is situated in the cytoplasm, a time τ_{step} is added to the total time t . If the walker is active and situated in the region with the native DNA, then a random time is added to t . This latter random time is taken from an exponential distribution with average $\tau_{\text{step}}(1 + K_{\text{ns}}^0I_{\text{DNA}}^{(1)})$.
2. One of the 6 directions possible on a cubic lattice is chosen at random. If a bond exists to a neighbouring site in this direction, the walker moves to this site, otherwise it stays put.
3. If the walker is in the active state, it switches with probability $1/5$ to the inactive state. If instead the walker is in the inactive state, it switches to the active state with probability $x_{\text{act}}/5/(1 - x_{\text{act}})$. In the case when $x_{\text{act}} = 1$, this switching is turned off and the walker always stays in the active state.
4. If the walker is on the target site and in the active state, the target is considered to be found, and the time t is recorded as the search time. Otherwise the iteration goes back to step 1.

This procedure is repeated 5,000 times on the same percolation cluster, but with a new target position and initial position of the searcher each time. The MFPT is calculated as the average of the 5,000 recorded search times.

References

- [1] See, for instance, P. H. von Hippel and O. G. Berg, *J. Biol. Chem.* **264**, 675 (1989). For a recent example investigating EcoRV, see Ref. [23] and M. A. Lomholt et al., *Proc. Natl. Acad. Sci. USA* **106**, 8204 (2009).
- [2] A. P. Minton, *J. Cell Science* **199**, 2863 (2006); H. Zhou, G. Rivas, and A. P. Minton, *Ann. Rev. Biophys.*, **37**, 375 (2008); J. A. Dix and A.S. Verkman, *Ann. Rev. Biophys.*, **37**, 247 (2008).
- [3] S. B. Zimmerman and S. O. Trach, *J. Mol. Biol.* **222**, 599 (1991). H. Dong, S. Qin, H.-X. Zhou, *PLoS Comp. Biol.* **6**, e1000833 (2010). R. J. Ellis and A. P. Minton, *Nature*, **425**, 27 (2003). R. J. Ellis, *Trends Biochem. Sci.* **26**, 597

- (2001). S. B. Zimmerman and A. P. Minton, *Annu. Rev. Biophys. Biomol. Struct.* **22**, 27 (1993).
- [4] D. ben-Avraham and S. Havlin, *Diffusion and Reactions in Fractals and Disordered Systems* (Cambridge University Press, Cambridge, UK, 2005).
- [5] C. D. Lorenz and R. M. Ziff, *Phys. Rev. E* **57**, 230 (1998).
- [6] S. R. McGuffee and A. H. Elcock, *PLoS Comput. Biol.* **6**, e1000694 (2010).
- [7] G. Seisenberger et al., *Science* **294**, 1929 (2001).
- [8] M. Weiss, M. Elsner, F. Kartberg, and T. Nilsson, *Biophys. J.* **87**, 3518 (2004).
- [9] I. Golding and E. C. Cox, *Phys. Rev. Lett.* **96**, 098102 (2006).
- [10] I. Bronstein et al., *Phys. Rev. Lett.* **103**, 018102 (2009).
- [11] S. C. Weber, A. J. Spakowitz, and J. A. Theriot, *Phys. Rev. Lett.* **104**, 238102 (2010).
- [12] J.-H. Jeon et al., *Phys. Rev. Lett.* **106**, 048103 (2011).
- [13] D. Banks and C. Fradin, *Biophys. J.* **89**, 2960 (2005).
- [14] W. Pan et al., *Phys. Rev. Lett.* **102**, 058101 (2009).
- [15] J. Szymanski and M. Weiss, *Phys. Rev. Lett.* **103**, 038102 (2009).
- [16] G. Guigas and M. Weiss, *Biophys. J.* **94**, 90 (2008).
- [17] G. Kolesov et al., *Proc. Natl. Acad. Sci. USA* **104**, 13948 (2007).
- [18] M. A. Lomholt, I. M. Zaid, and R. Metzler, *Phys. Rev. Lett.* **98**, 200603 (2007); I. M. Zaid, M. A. Lomholt, and R. Metzler, *Biophys. J.* **97**, 710 (2009).
- [19] A. Jeltsch, C. Wenz, F. Stahl, and A. Pingoud, *EMBO J.* **15**, 5104 (1996).
- [20] A. Pingoud, M. Fuxreiter, V. Pingoud, and W. Wende, *Cell. Mol. Life Sci.* **62**, 685 (2005).
- [21] S. G. Erskine, G. S. Baldwin, and S. E. Halford, *Biochem.* **36**, 7567 (1997).
- [22] F. K. Winkler et al., *EMBO J.* **12**, 1781 (1993).
- [23] B. v. d. Broek et al., *Proc. Natl. Acad. Sci. USA* **105**, 41, 15738 (2008).
- [24] A. D'Arcy et al., *J. Biol. Chem.* **260**, 1987 (1985).
- [25] R. Cuthbertson, W. M. L. Holcombe, and R. Paton, *Computation in cellular and molecular biological systems* (World Scientific, Singapore, 1995).
- [26] See Supplementary Material.
- [27] M. J. Saxton, *J. Chem. Phys.* **116**, 203 (2002).
- [28] C. Loverdo, O. Bénichou, and R. Voituriez, *Phys. Rev. Lett.* **102**, 188101 (2009).
- [29] C. C. Fritsch and J. Langowski, *J. Chem. Phys.* **133**, 025101 (2010).
- [30] Similar insights into the effect of crowding environments were obtained from lattice random walks and off-lattice Brownian dynamics simulations in J. D. Schmit, E. Kamber, and J. Kondev, *Phys. Rev. Lett.* **102**, 218302 (2009); N. Dorsaz et al., *Phys. Rev. Lett.* **105**, 120601 (2010).
- [31] I. Bonnet et al., *Nucleic Acids Res.* **36**, 4118 (2008).
- [32] J. Elf, G.-W. Li, X. S. Xie, *Science* **316**, 1191 (2007).
- [33] A. Jeltsch and A. Pingoud, *Biochemistry* **37**, 2160 (1998).
- [34] B. D. Hughes, *Random Walks and Random Environments*, Vol. 1 (Oxford University Press, Oxford, UK, 1995).
- [35] S. Condamin, O. Bénichou, V. Tejedor, R. Voituriez, and J. Klafter, *Nature* **450**, 77 (2007).
- [36] J.-H. Jeon, A. V. Chechkin, and R. Metzler, *EPL* **94**, 20008 (2011).
- [37] For a recent summary, see, e.g., S. Burov, J.-H. Jeon, R.

Metzler, and E. Barkai, Phys. Chem. Chem. Phys. **13**, 1800 (2011).